**Structural Engineering and Mechanics**, *Vol. 60, No. 3 (2016) 365-386*
DOI: http://dx.doi.org/10.12989/sem.2016.60.3.365 

# Effects of imperfection shapes on buckling of conical shells under compression

Meisam Shakouri*[1], Andrea Spagnoli[2a] and M.A. Kouchakzadeh[3b]

[1]*Department of Aerospace Engineering, Semnan University, Semnan, Iran*
[2]*DICATeA, University of Parma, Parco Area delle Scienze 181/A, 43124 Parma, Italy*
[3]*Department of Aerospace Engineering and Center of Excellence in Aerospace Systems, Sharif University of Technology, P.O. Box 11155-8639, Tehran, Iran*

*(Received January 8, 2016, Revised July 13, 2016, Accepted July 28, 2016)*

**Abstract.** This paper describes a systematic numerical investigation into the nonlinear elastic behavior of conical shells, with various types of initial imperfections, subject to a uniformly distributed axial compression. Three different patterns of imperfections, including first axisymmetric linear bifurcation mode, first non-axisymmetric linear bifurcation mode, and weld depression are studied using geometrically nonlinear finite element analysis. Effects of each imperfection shape and tapering angle on imperfection sensitivity curves are investigated and the lower bound curve is determined. Finally, an empirical lower bound relation is proposed for hand calculation in the buckling design of conical shells.

**Keywords:** buckling; conical shell; imperfection sensitivity; weld depression

## 1. Introduction

Geometric imperfections have long been recognized as the main factor influencing the decrease of the buckling load for thin walled shells.

Effect of imperfections on instability of cylindrical shells has extensively been studied by many authors. It is well known from buckling experiments of shells that the actual failure load might be significantly lower (depending on loading conditions) than the buckling load obtained from linear eigenvalue (bifurcation) analysis (Falzon and Aliabadi 2008), due to the presence of local or global imperfections in the nominal geometry of the shells. The first significant works by von Kármán and Tsien (1941), Donnell and Wan (1950), Koiter (1970) identified deviations from the idealized geometry of a shell, known as initial geometric imperfections, as a primary source of variation between analytical predictions and experimental results.

Chadhuri and Kim (2008) studied buckling response of a thin cross-ply cylindrical shell with localized imperfection under external pressure.

It is known that the most important factor in imperfection sensitivity of the shell is the

∗Corresponding author, Assistant Professor, E-mail: shakouri@semnan.ac.ir
[a]Professor, E-mail: spagnoli@unipr.it
[b]Professor, E-mail: mak@sharif.edu

**Copyright © 2016 Techno-Press, Ltd.**
http://www.techno-press.org/?journal=sem&subpage=8 ISSN: 1225-4568 (Print), 1598-6217 (Online)

membrane component of strain energy and axial compression is the loading condition allowing the shell to develop a high membrane component of the total strain energy, which will result in higher imperfection sensitivity (Calladine 1995, Croll 1995). As a result, axial compression is the loading condition which has been mostly investigated (Jamal, Lahlou *et al*. 1999, Jamal, Midani *et al*. 2003, Song, Teng *et al*. 2004, Ali, Jalal *et al*. 2011, Castro, Zimmermann *et al*. 2014). Shultz and Nemeth (2010) presented an analytical model for assessing the imperfection sensitivity of axially compressed orthotropic cylinders and compared the results with those obtained through Finite Element (FE) models. Effects of single (Jamal, Lahlou *et al*. 1999) and multiple (Ali, Jalal *et al*. 2011) local dimple-shaped imperfections on the stability of cylindrical shells under axial compression were studied, showing that the more is the interaction of geometric imperfections the higher is the reduction of the buckling load. Castro, Zimmermann *et al*. (2014) performed FE analyses to study the effects of different geometric imperfection patterns on buckling of laminated cylindrical shells and compare the results with the lower-bound methods NASA SP-8007 (Peterson, Seide *et al*. 1968) and the Reduced Stiffness Method (RSM) (Batista and Croll 1980), showing that the axisymmetric imperfections give the lowest so-called knock-down factor.

Effect of imperfections on conical shells is less studied with respect to cylinders. Former investigations prove that there is imperfection sensitivity in conical shells subject to axial compression (Lackman and Penzien 1960, Spagnoli 2001, Chryssanthopoulos, Pariatmono *et al*. 1997, Spagnoli and Chryssanthopoulos 1999). Shiau and Soong (1974) used Galerkin approach to determine the dynamic stability of a truncated conical shell with various geometrical imperfections and dynamic loading conditions and showed that conical shells are less sensitive to initial geometric imperfections than the cylinders. Goldfeld (Goldfeld 2007) considered the sensitivity of laminated conical shells to imperfection via the initial post-buckling analysis, on the basis of Donnell, Sanders, and Timoshenko shell theories. Maali, Showkati *et al*. (2012) tested complete conical shells having meridional weld-induced imperfections and compared the results with FE analyses, and Sofiyev (Sofiyev 2011) studied the influence of initial imperfection on the buckling response of simply-supported truncated conical shells made of functionally graded materials under axial compression. Steel conical shells have long been used in various parts of different structures. The stability of composite conical shells subjected to dynamic external pressure is investigated both numerically and experimentally by (Jalili, Zamani *et al*. 2014). (Ghazijahani, Jiao *et al*. 2015) provide experimental data on the effect of local imperfections on the buckling capacity of these shells under axial compression. The results show changes in the buckling mode and the capacity for such damaged thin specimens with an average overall capacity reduction of 11%. However, effects of various types of imperfections on buckling strength of conical shells needs more study.

The main objectives of the present paper are: determine the type of imperfection pattern which is most critical in terms of load carrying capacity of conical shells, bearing in mind that in cylinders, weld depression is the most critical one (Rotter and Teng 1989); study the effects of tapering angle on imperfection sensitivity of the conical shells.

To this end, buckling and postbuckling behavior of conical shells under axial compression with various types of initial imperfection is studied. Three different patterns of imperfections are studied using geometrically nonlinear FE analysis. Effects of each imperfection shape and tapering angle on imperfection sensitivity curves are investigated and the lower bound curve is found. Finally, an empirical lower bound relation is proposed for hand calculation in the buckling design of conical shells.

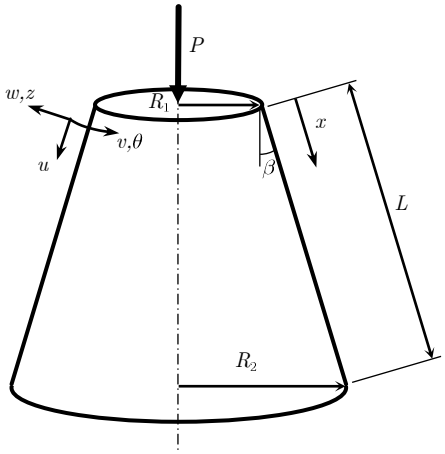


Fig. 1 Geometry of conical shell.

## 2. Finite element analysis

### *2.1 Geometry and material properties*

Consider a conical shell with ($x$, $\theta$, $z$) coordinates as shown in Fig. 1, where $x$ is the coordinate along the cone generator with the origin placed at the top, $\theta$ is the circumferential coordinate and $z$ is the coordinate normal to the cone surface. $R_1$ and $R_2$ are the radii of the cone at its small and large end, respectively, $\beta$ is the tapering angle of cone and $L$ is the cone slant length along the generator. The thickness of the cone is $t$.

The uniformly distributed axial load $P$ is applied along the small end of the shell. The material is assumed to be isotropic and linear elastic, with a Young's modulus $E$=200 GPa and a Poisson's ratio $\nu$=0.3, which are typical values for steel.

### *2.2 Finite element model*

All the numerical analyses were conducted using the ANSYS program (Lawrence 2012). Both shell ends were simply supported so that all translational degrees of freedom $w$, $u$ and $v$ were restrained on the bottom edge, while the axial displacement was left free on the top edge ($u\cos\beta - w\sin\beta \neq 0$) where the axial compressive force is applied. A complete-structure model was used to avoid any restriction which may be caused by symmetry assumption as discussed by Teng and Song (Teng and Song 2001).

The geometric parameters being considered in the study include the length, radius and tapering angle of cone, as well as the form, amplitude and position of geometric imperfections. The geometric imperfections were all represented by a complete definition of the imperfect shape, using doubly curved shell elements to capture local shell forms and ensure geometric and deformation compatibility between elements. Appropriate care was taken with mesh refinement where the imperfect geometry led to high local curvatures. The shell was assumed to be stress free in its imperfect geometry, since studies of consistent residual stresses in shells (Holst, Rotter *et al*. 2000) suggest that residual stresses are generally small and usually beneficial to the shell buckling

strength under axial compression.

### 2.3 Type of analysis

Following the guidelines of ECCS technical committee (Rotter and Schmidt 2008), linear eigenvalue buckling (bifurcation) analyses (LBA) present the reference buckling loads for all conditions, as well as they give mode shapes which are in general detrimental when used as geometric imperfections. Geometrically nonlinear elastic analyses using different representation of geometric imperfections (GNIA) is then carried out to obtain bifurcation and limit load points for the imperfect structure.

The nonlinear load-deflection path was followed using the arc length method (Riks 1979). In this method, the algorithm looks for successive points on the load-deformation path of the loaded structure. This method is very powerful for studying shell buckling, where these stiff light structures support very high loads, but can easily transform into rapidly collapsing systems. A full Newton-Raphson solution is conducted on an incremental basis, and during each increment, iterations are performed so that equilibrium between external and internal forces is achieved at the end of the step. Then, the determinant of the stiffness matrix was checked at each step to determine if one or more negative eigenvalues had appeared. The appearance of a negative eigenvalue indicates that a bifurcation point on the load-deflection path has been passed. The buckling loads reported in the nonlinear analyses correspond to the peak points along the geometrically nonlinear path.

### 2.4 Shell elements

Due to the quadratic representation of the curved surface, the 8-node isoparametric shell element SHELL281 of ANSYS involving both bending and membrane effect is adopted. This kind of shell element is such that the membrane and bending locking and spurious energy mode do not occur in analysis, e.g., see (Nascimbene 2014). Each element node has in total six translations and rotations degrees of freedom (DOFs), and the accuracy is governed by the first order shear deformation theory.

### 2.5 Mesh study

Several mesh convergence studies were conducted. A good approach, base on h-convergence, for such studies is to adopt a mesh which provides almost identical results to those from a further refined mesh (i.e., the buckling load is changed by less than 1% as a result of the mesh size bisection). This study followed this approach. Since we want to undertake parametric studies of the buckling and post-buckling behavior of cylindrical and conical shells with and without imperfections, the mesh convergence study aimed to find meshes that predict both the buckling and the post-buckling behavior accurately, without excessive computing effort. Appropriate attention was paid to mesh refinement in the imperfection zones (especially weld depressions), since careful definition of the doubly curved geometry of a local imperfection is essential to an accurate determination of the buckling strengths of locally imperfect shells.

Since the deformation path of nonlinear finite element analysis of shell calculated using the arc-length method can be sensitive to the maximum arc-length increment at each load step (Teng and Song 2001) and lower arc-length increments increase the calculation time gradually, the maximum

Table 1 Mesh convergence study for cylinder with $L/R_1$=2, $R_1/t$=500, and $t$=1 mm

| Mesh name | Nodal spacing (circ.,merid.) | $P_{cr}^{L}$ (MN) | $P_{max}/P_{cr}^{L}$ |
|---|---|---|---|
| A | (1.5°,3 $\lambda_{cl}$/8) | 761.452 | 0.921 |
| B | (1°, $\lambda_{cl}$/4) | 759.024 | 0.842 |
| C | (0.75°,3 $\lambda_{cl}$/16) | 756.483 | 0.843 |
| D | (0.5°, $\lambda_{cl}$/8) | 755.871 | 0.843 |

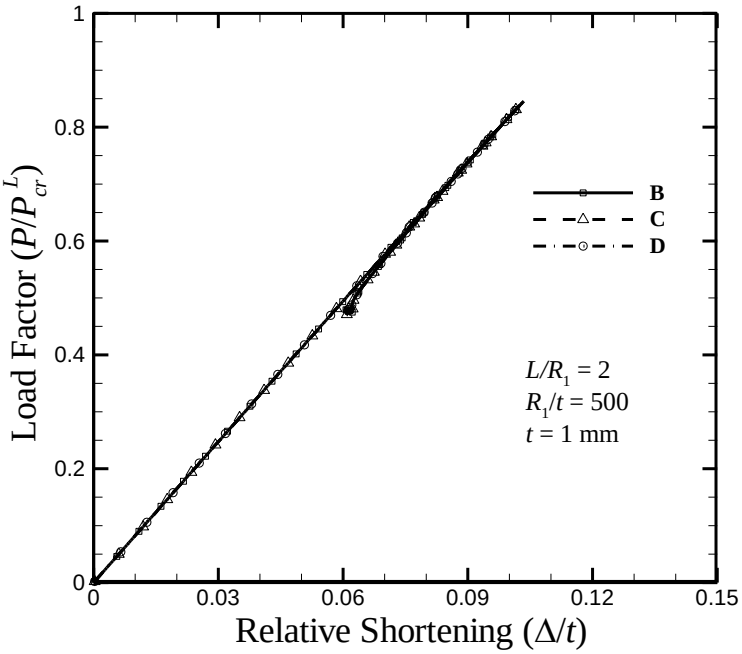


Fig. 2 Load-deflection curves for various mesh sizes of the perfect cylinder under axial compression

arc-length increment is set to 2.

For shell buckling and post-buckling analysis, discretization into finite elements is best discussed in terms of the number of elements or nodes per half-wavelength of the relevant bending or buckling deformations (which are also considered as characteristic deformation of imperfection geometries). In the present study, the (minimum) half-wavelength $\lambda_{cl}$ for a cone with axisymmetric buckling mode

$$\lambda_{cl} = 1.728\sqrt{\rho_1 t}, \qquad \rho_1 = \frac{R_1}{\cos\beta} \tag{1}$$

was considered.

### *2.5.1 Mesh convergence for cylinders*

At first, finite element analyses were obtained using three different meshes for a cylinder with $L/R_1$=2, $R_1/t$=500, and $t$=1 mm. The meshes are described in terms of the circumferential nodal spacing in degrees and the meridional nodal spacing as a fraction of the half-wavelength $\lambda_{cl}$ (Song *et al*. 2004).

The linear bifurcation buckling load $P_{cr}^{L}$ and the limit point load on the geometrically nonlinear path $P_{max}$ of the perfect shell are listed in Table 1. The mesh A is not fine enough to predict the nonlinear limit load correctly. Since the values change less than 1% on other mesh sizes, meshes B, C and D are adequate. In addition, the calculated post-buckling path (Fig. 2) is followed by B, C and D, indicating that the mesh B is satisfactory. In Fig. 2, the horizontal axis is the relative shortening (i.e., the axial shortening ($\Delta$) divided by the shell thickness), while the vertical axis is the load factor (i.e., the axial load $P$ divided by the linear bifurcation buckling load ($P_{cr}^{L}$)).

### *2.5.2 Mesh convergence for cones*

The same convergence approach is used to study the adequate mesh sizes for a cone with $L/R_1$=2, $R_1/t$=500, $t$=1 mm and $\beta$=30°.The results are collected in Table 2. Also, the post-buckling path is shown in Fig. 3. It can be seen that the mesh B cannot follow the second path of C and D. This may be due to its coarseness or the maximum arc-length increment chosen for this problem (Song *et al*. 2004). In addition, by applying mesh C the analyses were performed in reasonable time but mesh D is very fine and calculation time becomes very high.

Hence, the mesh size C is appropriate for both cylinders and cones. The following calculations are performed using this size.

Table 2 Mesh convergence study for cone with $L/R_1$=2, $R_1/t$=500, $t$=1 mm and $\beta$=30°

| Mesh name | Nodal spacing (circ.,merid.) | $P_{cr}^{L}$ (kN) | $P_{max}/P_{cr}^{L}$ |
|---|---|---|---|
| A | (1.5°,3 $\lambda_{cl}$/8) | 570.49 | 0.871 |
| B | (1°, $\lambda_{cl}$/4) | 569.71 | 0.842 |
| C | (0.75°,3 $\lambda_{cl}$/16) | 567.24 | 0.843 |
| D | (0.5°, $\lambda_{cl}$/8) | 566.89 | 0.843 |

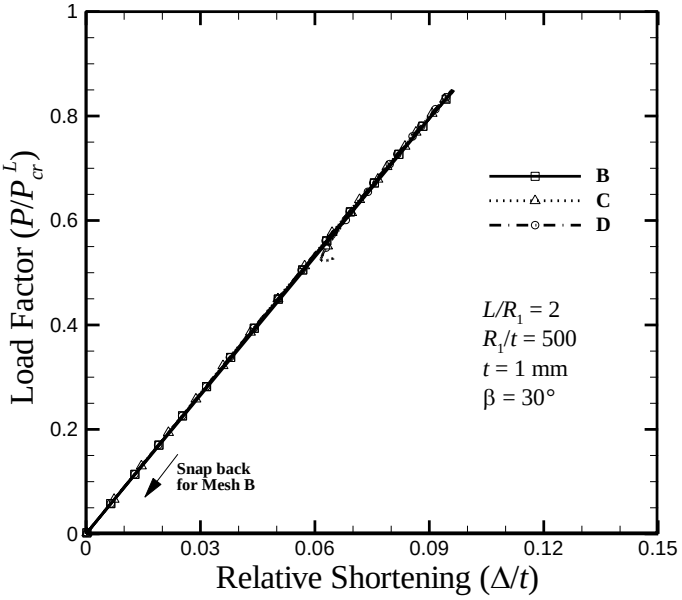


Fig. 3 Load-deflection curves for various mesh sizes of the perfect cone under axial compression

## 3. Imperfection forms

The load-carrying capacity of an axially compressed conical shell is strongly influenced by the distribution and amplitude of geometric imperfections in the shell. As discussed by Teng and Rotter (2004), different alternative choices were proposed from time to time by researchers who were looking for practical but severe forms of imperfection for axially compressed cylinders. Yamaki (1984) explored many different imperfection forms for cylinders. However, a comprehensive study of the effects of imperfection forms in the buckling of axially compressed cones is still missing.

The discrepancy between classical buckling stress predictions and experimental buckling strengths was first shown to be predominantly caused by geometric imperfections in the shell surface by Koiter (1970) in 1945. His perturbation analysis explored the effect on the buckling stress of minor deviations in geometry in the form of the axisymmetric buckling mode with wavelength $\lambda_{cl}$. This original analysis for a long cylinder with sinusoidal imperfections throughout its length led to the simple asymptotic formula for the buckling load (stress) at bifurcation as

$$P_{max} = P_{cr}^{L}\left\{1 - \frac{3}{4}\psi\delta\left[\left(1 + \frac{8}{3\psi\delta}\right)^{\frac{1}{2}} - 1\right]\right\} \tag{2}$$

where $\psi$ is a constant defined as

$$\psi = \sqrt{3(1-\nu^2)} \simeq 1.652 \tag{3}$$

and $\delta$ is the relative imperfection amplitude defined as

$$\delta = \frac{w_0}{t} \tag{4}$$

where $w_0$ is the imperfection value, measured as a normal-to-shell-wall deviation from the nominal surface.

Koiter showed that imperfections in the form of axisymmetric buckling mode for the perfect cylinder, may be regarded as the most serious for the strength of the shell, leading to a reduction to 24% of the classical critical stress for an amplitude of one wall thickness ($\delta$ =1). Koiter introduced his next formula for imperfection sensitivity including the effects of non-symmetric modes in 1970 (Hutchinson and Koiter 1970, Koiter and Heijden 2009) as follows

$$(1 - \frac{P_{max}}{P_{cr}^{L}})^{\frac{3}{2}} = \frac{3}{2}\psi\frac{P_{max}}{P_{cr}^{L}}\delta \tag{5}$$

Also, Yamaki (1984) introduced some curves for imperfection sensitivity of long cylinders. In this paper we use Eq. (4.7.C) from (Yamaki 1984) as

$$(1 - \frac{P_{max}}{P_{cr}^{L}})^{\frac{3}{2}} = \frac{3}{2}\sqrt{-3b_2}\left[I_1 - \left(1 - \frac{P_{max}}{P_{cr}^{L}}\right)J_1\right]\delta \tag{6}$$

where

$$b_2 = -0.87,\ I_1 = 0.54,\ J_1 = 0.85 \tag{7}$$

In this study, three types of imperfection forms were considered: the first non-axisymmetric linear bifurcation mode (FNLB), the first axisymmetric linear bifurcation mode (FALB), and local weld depressions (WD).

Table 3 Mode number, corresponding meridional and circumferential wave numbers (*m*,*n*) and corresponding linear buckling loads of FNLB and FALB forms.

| Tapering Angle | FNLB | FALB | $P_{FNLB}$ (kN) | $P_{FALB}/P_{FNLB}$ |
|---|---|---|---|---|
| 0 | 1(14,20) | 51(13,0) | 756.5 | 1.004 |
| 15 | 1(18,20) | 43(23,0) | 706.1 | 1.006 |
| 30 | 1(18,19) | 27(19,0) | 567.2 | 1.005 |
| 45 | 1(16,17) | 27(16,0) | 378.4 | 1.004 |
| 60 | 1(11,14) | 21(14,0) | 189.3 | 1.005 |

### *3.1 Linear bifurcation modes*

The linear bifurcation mode of the perfect shell has long been used (Koiter 1963, Koiter 1970, Yamaki 1984) as an equivalent imperfection form, because it is easily obtainable and generally gives a relatively severe form of imperfection (Rotter and Schmidt 2008). Here, the first axisymmetric and non-axisymmetric bifurcation modes are selected to study the effects of the imperfection shape on post-buckling path and imperfection sensitivity of cylinders and cones. Table 3 shows the mode number, corresponding meridional and circumferential wave numbers (*m*,*n*) and corresponding buckling loads of FNLB and FALB forms. The meridional wave number (*m*) is the number of half wavelengths in meridional direction while the circumferential wave number (*n*) is the number of full wavelengths in circumferential direction. As can be seen, the first mode is the non-axisymmetric mode for all the tapering angles. The first axisymmetric mode is not the overall first mode, but its buckling load is extremely close to the first mode of buckling. This is due to the cluster of simultaneous buckling modes in cylinders and cones that has thoroughly been discussed elsewhere (Spagnoli 2001, Spagnoli 2003, Shakouri *et al*. 2014).

#### *3.1.1 First non-axisymmetric linear bifurcation mode (FNLB)*

For the range of geometries being considered, the FNLB mode is always the first buckling mode of the shell according to Table 3. Fig. 4 shows the initial post-buckling curves for a cylinder and cones with $L/R_1$=2, $R_1/t$=500, $t$=1 mm and different values of tapering angles.

The imperfection sensitivity curve of cones and the comparison with the results for the cylinders obtained by Koiter (Hutchinson and Koiter 1970, Koiter 1970) and Yamaki (1984) are shown in Fig. 5. Accordingly, it can be concluded that the cone response to imperfection is similar to that of cylinders, so that the use of "equivalent cylinder" concept appears to be reasonable. In this concept, the design procedure for a cone or truncated cone is transformed into the buckling strength verification of an equivalent cylinder of length $l_e$ and radius $r_e$, as has confirmed by many researchers including Esslinger and Ciprian (1982), Pariatmono and Chryssanthopoulos (1995) for elastic and also Blachut (2011) for elasto-plastic behavior of conical shells under axial compression.

In most of the cases, as seen in Fig. 4, the load-displacement curve reaches a peak value which can be selected as the failure state and chosen as the maximum load factor. In some cone geometries and imperfection amplitudes, there is no a distinct peak value to be chosen as the maximum load factor and identifying the failure in these cases needs more care. Three possible criteria of failure are introduced in ECCS guideline (Rotter and Schmidt 2008) (see sec. 8.1.1.17) as limit load, bifurcation point and the largest tolerable deformation. These conditions are used to find the correct values for load factors.

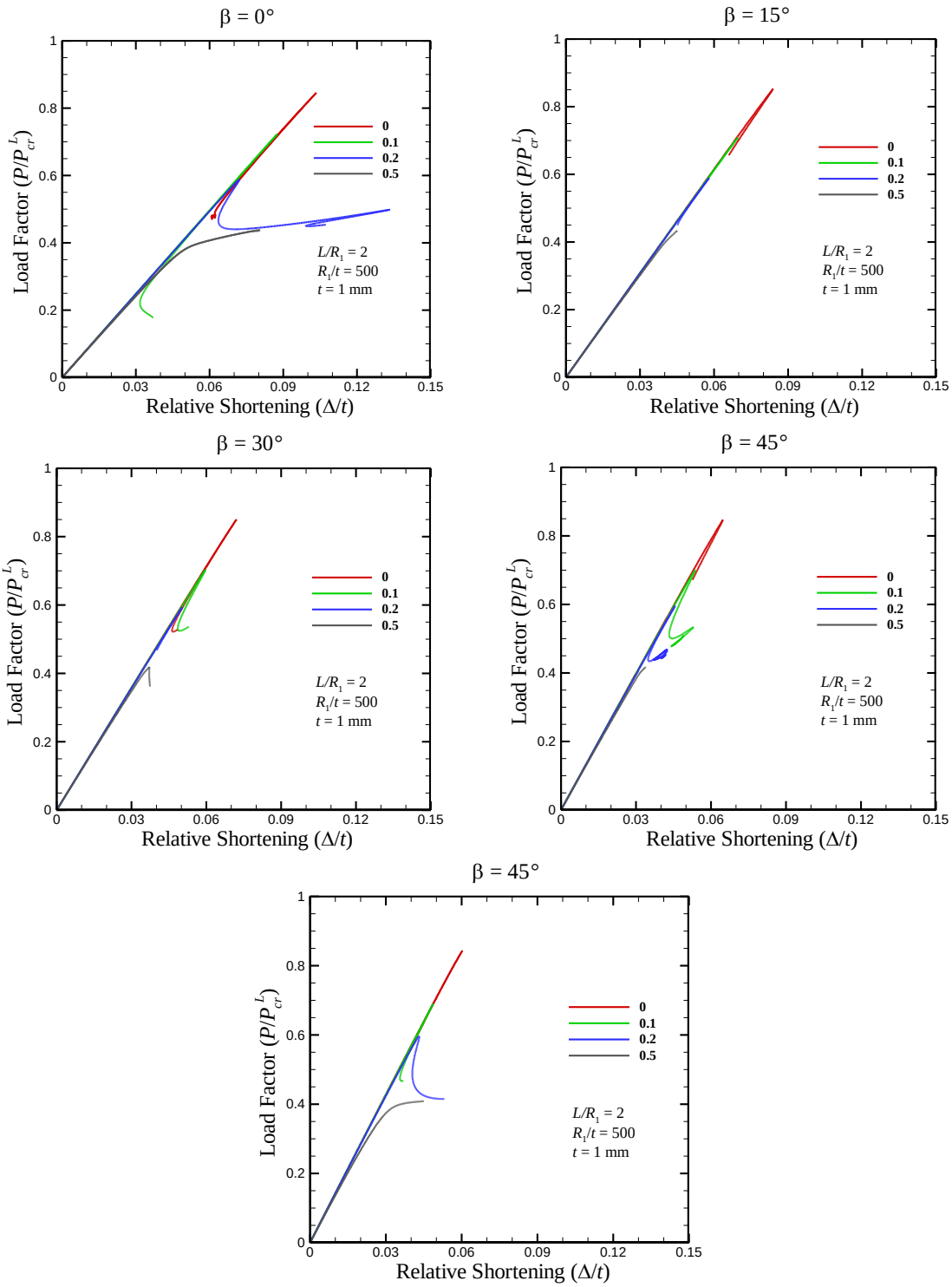


Fig. 4 Initial post-buckling curves of the imperfect cylinder and cones with various tapering angles and different relative amplitude of imperfections

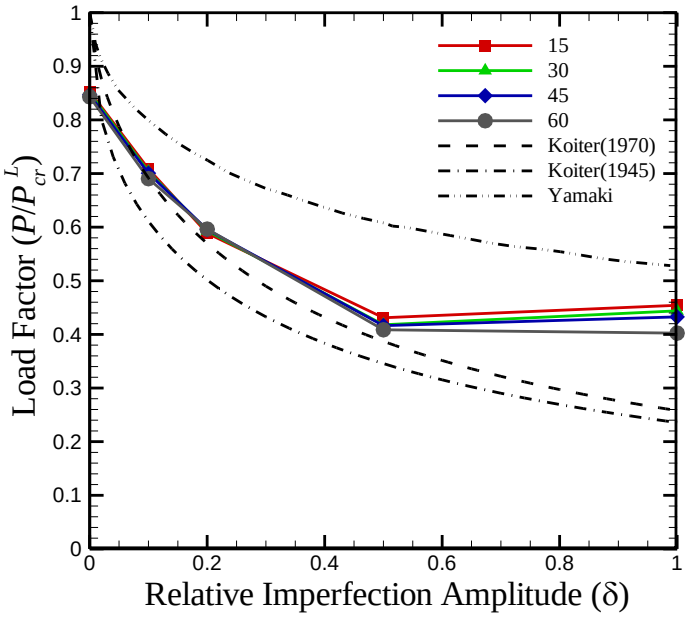


Fig. 5 Imperfection sensitivity curves for imperfect cones with FNLB mode

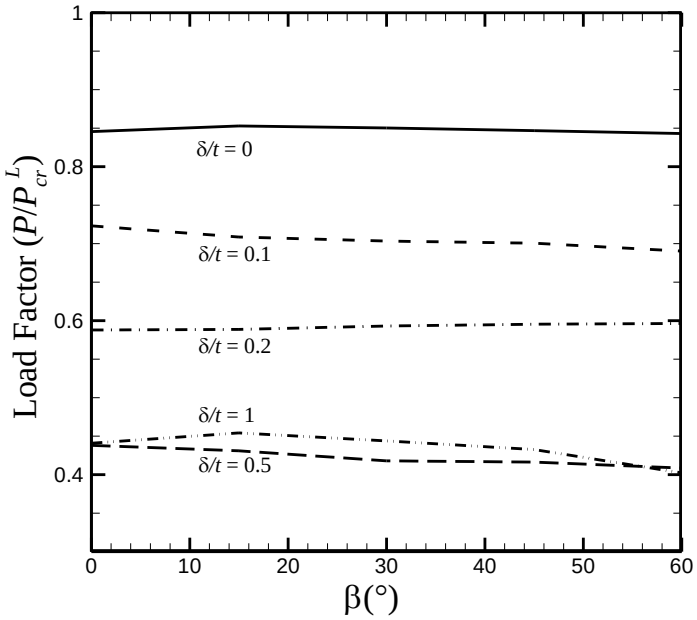


Fig. 6 Effect of tapering angle of the cone on imperfection sensitivity of cone analyzed using FNLB mode

The effect of tapering angle on load bearing capacity of the cones with various values of imperfection amplitude is shown in Fig. 6. As can be seen, the tapering angle produces a negligible influence on the imperfection sensitivity.

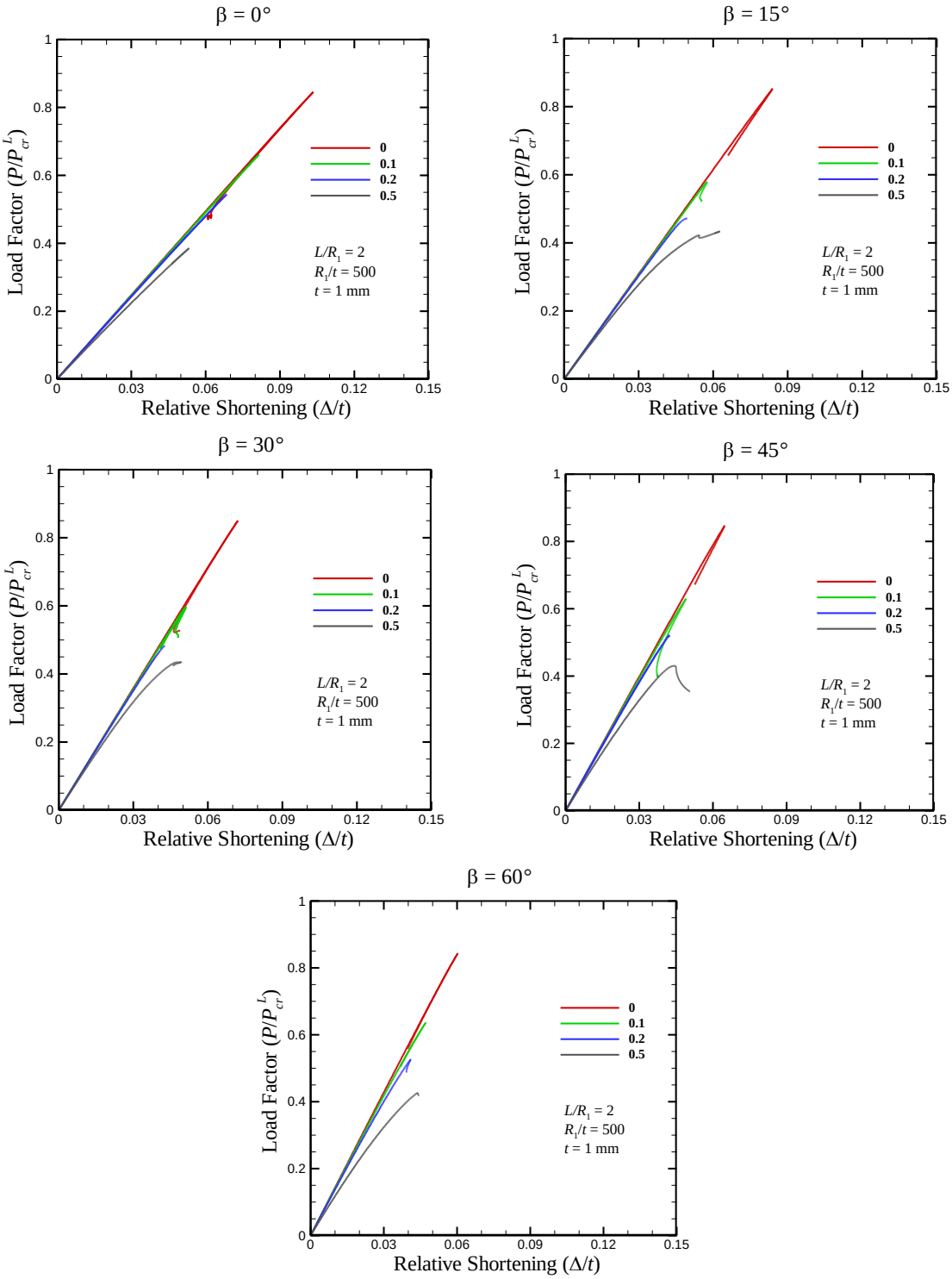


Fig. 7 Initial post-buckling curves of the FALB imperfect cones with various tapering angles and different relative amplitude of imperfections

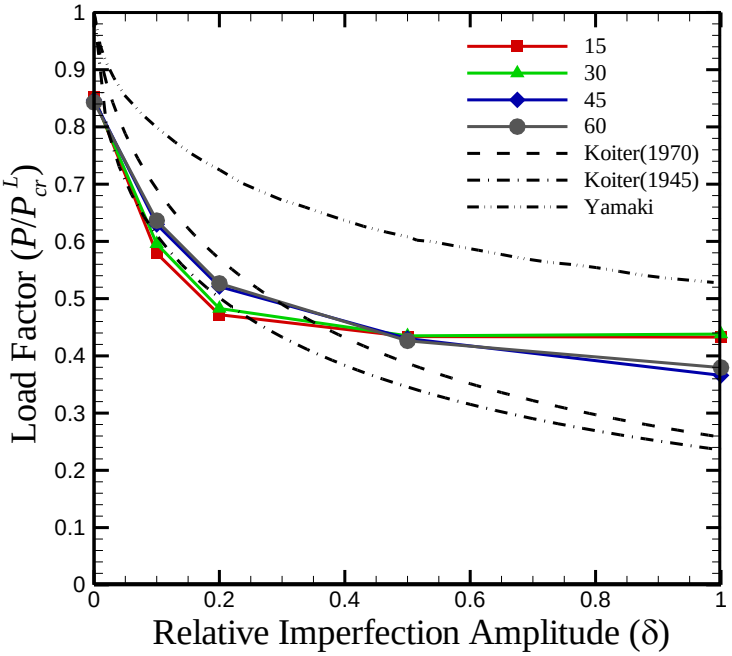


Fig. 8 Imperfection sensitivity curves for imperfect cones with FALB mode

### *3.1.2 First axisymmetric linear bifurcation mode (FALB)*

According to Table 3, the first axisymmetric mode is used as initial imperfection on the shell. Fig. 7 shows the initial post-buckling curves for a cylinder and cones with $L/R_1$=2, $R_1/t$=500, $t$=1 mm and various values of tapering angles.

The imperfection sensitivity curve of cones and the comparison with the results for the cylinders obtained by Koiter (Hutchinson and Koiter 1970, Koiter 1970) and Yamaki (1984) are shown in Fig. 8.

The effect of tapering angle on imperfection sensitivity of the cones with various values of imperfection amplitude is shown in Fig. 9. As can be seen, the tapering angle has negligible changes on the imperfection sensitivity.

### *3.2 Weld depressions*

This weld (sinusoidal) imperfection was explored by Muggeridge and Tennyson (1969), who found that the critical imperfection wavelength varies with the imperfection amplitude. Imperfections in the form of linear bifurcation modes, nonlinear buckling modes and post-buckling deformed shapes are all idealized forms that are generally not encountered in real shell structures. Imperfections in real structures take different forms, the simplest and most easily recognizable of which is probably the axisymmetric weld depression (Rotter and Teng 1989). Teng and Rotter (1992) studied this form with a rigorous nonlinear analysis and found that the critical wavelength for amplitude equal to the thickness is 25% longer than the linear bending wave-length. Berry *et al*. (2000) measured the form of the weld imperfection in their fabricated specimens and found that the actual half-wavelength, with 90% confidence limits was given by

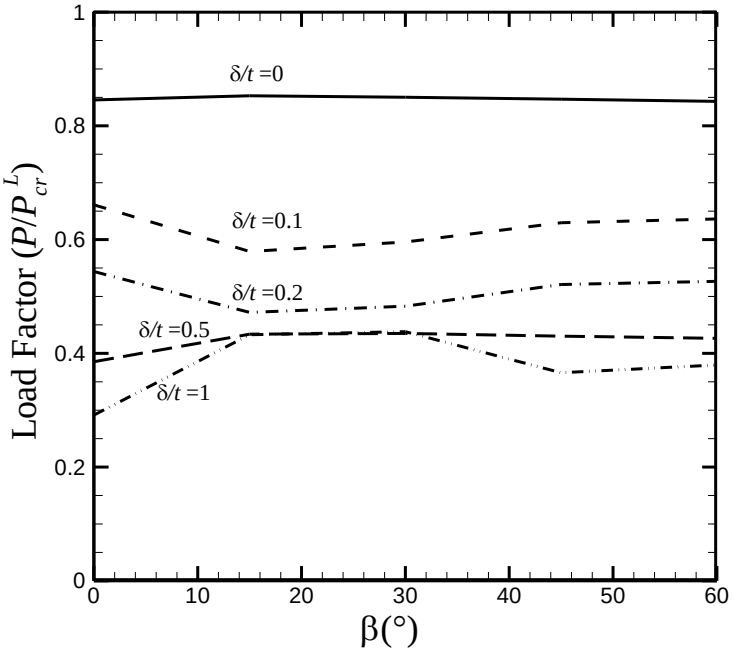


Fig. 9 Effect of tapering angle of the cone on imperfection sensitivity of cone analyzed using FALB mode

$$\lambda = (0.97 \pm 0.02)\lambda_b \tag{8}$$

where $\lambda_b$ is the linear elastic bending half-wavelength defined as

$$\lambda_b = \sqrt{2}\lambda_{cl} \simeq 2.444\sqrt{\rho_1 t} \tag{9}$$

The shape of the typical weld depression and its effect on the buckling strength under uniform axial compression has been studied using both theoretical and experimental methods by many authors (Rotter and Teng 1989, Ding, Coleman *et al*. 1996, Berry, Rotter *et al*. 2000, Pircher, Berry *et al*. 2001). Rotter and Teng (1989) proposed two limiting cases for the geometry, based on linear shell bending theory: the weld was either rotationally stiff during shrinkage (Type A) or rotationally free during shrinkage (Type B). The expression for the Type A weld depression was formulated using the above assumption and elastic shell bending theory for a long cylinder, namely (Rotter and Teng 1989)

$$w = \delta e^{-\left(\frac{\pi x}{\lambda_b}\right)}\left(\cos\frac{\pi x}{\lambda_b} + \sin\frac{\pi x}{\lambda_b}\right) \tag{10}$$

The Type A weld depression form is used in this study and the location of weld depression is assumed to be in the middle of the shell. Note that a weld depression imperfection could be placed in general anywhere throughout the meridian of conical shell. Under uniform compression for cylinders, the location is unimportant unless adjacent depressions cause interactions, or the weld is so close to an end boundary that the boundary conditions provide restraint, but in cones where a varying compressive stress field is involved, the location can strongly affect the strength (Rotter 1996). Accordingly, to obtain any general conclusion, information concerning the effect of weld

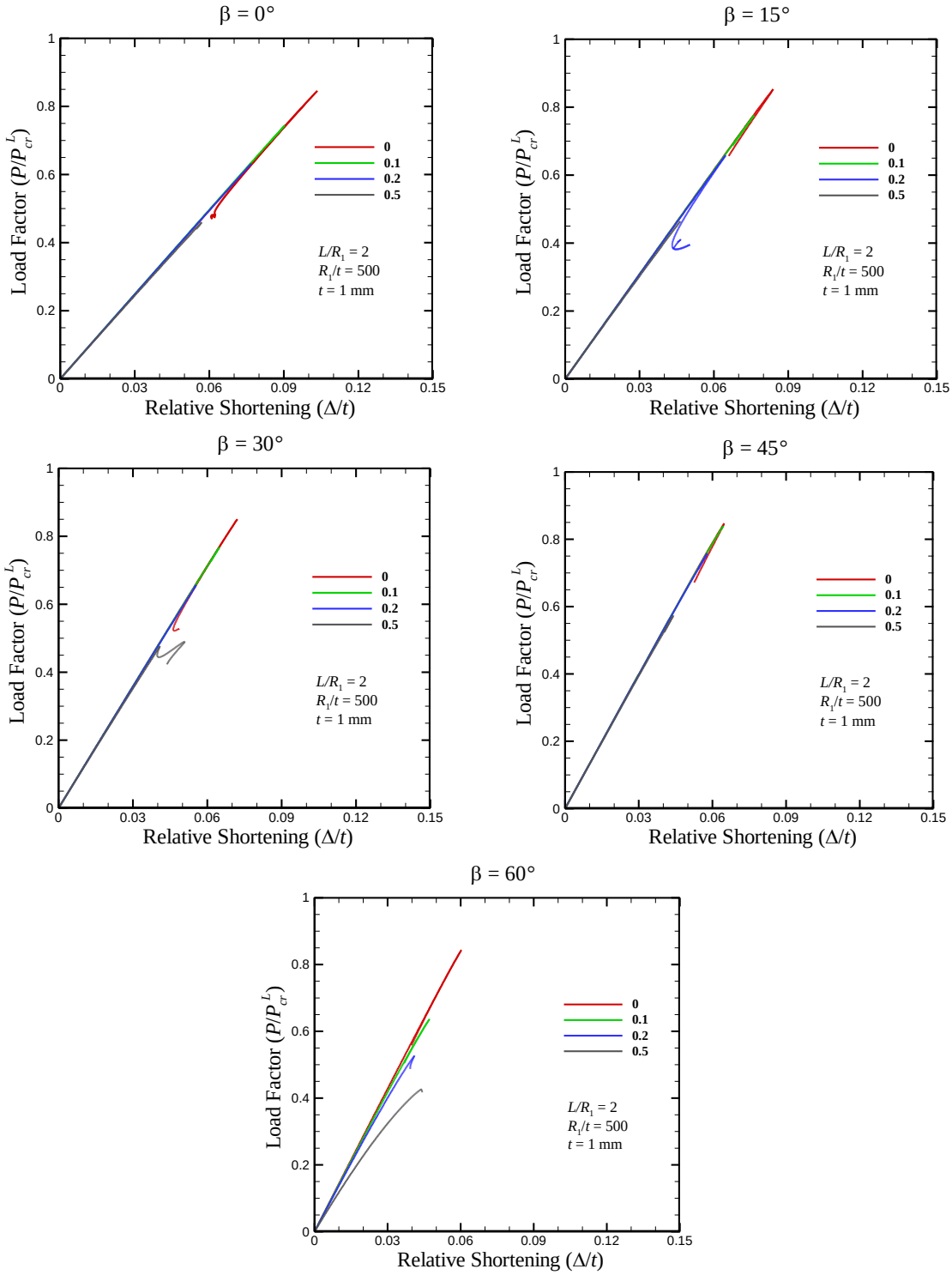


Fig. 10 Initial post-buckling curves of the weld depression imperfect cones with various tapering angles and different relative amplitude of imperfections

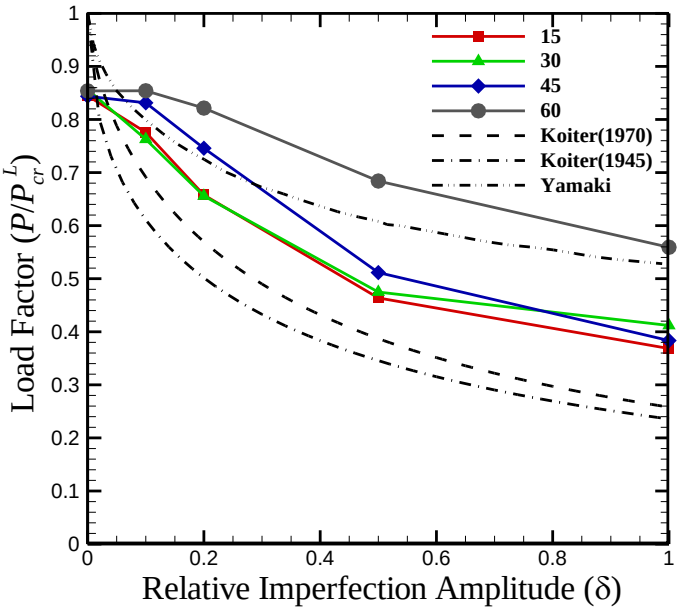


Fig. 11 Imperfection sensitivity curves for imperfect cones with WD mode

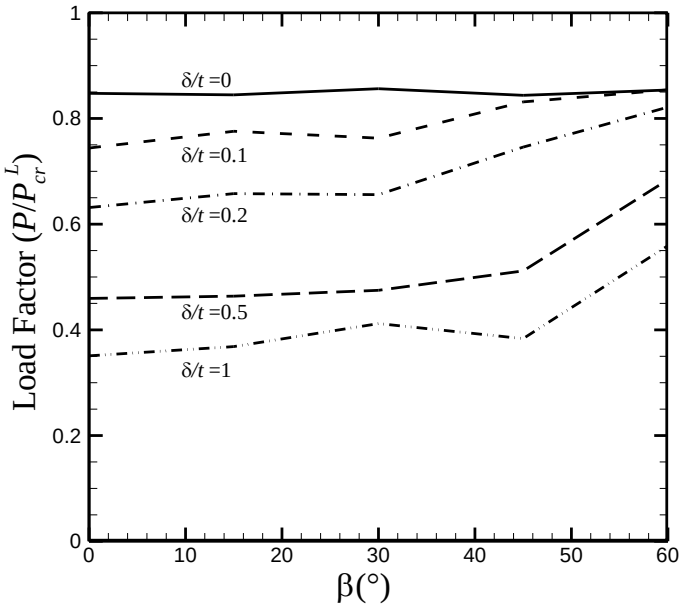


Fig. 12 Effect of tapering angle of the cone on imperfection sensitivity of cone analyzed using WD mode

depression location in conical shells should be further investigated.

Fig. 10 shows the initial post-buckling curves for a cylinder and cones with $L/R_1$=2, $R_1/t$=500, $t$=1 mm and various values of tapering angles with weld depression imperfection.

The imperfection sensitivity curve of cones and the comparison with the results for the

cylinders obtained by Koiter (Hutchinson and Koiter 1970, Koiter 1970) and Yamaki (1984) are shown in Fig. 11.

The effect of tapering angle on imperfection sensitivity of the cones with various values of imperfection amplitude is shown in Fig. 12. As can be seen, the effect of tapering angle is negligible for small angles and become more effective with increase of this value.

### *3.3 Imperfection measurement*

Since the buckling strength is very sensitive to the amplitude and form of geometric imperfections, amplitude of imperfections must be controlled by tolerance measures as part of the design process. However, a major difficulty arises here, as it is not easy for the designer to predict the level of imperfections which may be found in the structure, or for the fabricator to control the magnitude and shape of the imperfections being produced. Most design rules have been developed on the basis of empirical lower bounds of experimental results. Standards that have adopted this approach include API 620 (Standard 1977), AWWA D100 (Association 1984), ECCS (Rotter and Schmidt 2008) and DIN 18800 (Norm 1990). An effort to correlate this lower bound with appropriate tolerance measurements was made in the ECCS (Rotter and Schmidt 2008) and DIN (Norm 1990) standards, although a quantitative basis of the match has been publishedn elsewhere (Teng and Rotter 2004).

Inspired by the ECCS (Rotter and Schmidt 2008), to obtain the imperfection depth in conical shells, the following two measurements should be performed

1- Due to meridional compressive stresses, measurements of the depth $\Delta w_{0x}$ should be made. These tolerance measurements are chiefly conceived in the context of the buckling wavelength of the perfect shell, which has a half wavelength in each direction of $2\lambda_{cl}$ or about $3.5\sqrt{\rho_1 t}$. Since the value to be measured is not so precise, the normal measuring stick should have a length of

$$L_{gx} = 4\sqrt{\rho_1 t} \tag{11}$$

to reflect the classical eigenmode as shown in Fig. 13(a).

2- Additionally, measurements across welds of the depth $\Delta w_{0w}$ should be made using the gauge length $L_{gw}$ given by

$$L_{gw} = 25t \tag{12}$$

This measurement is additionally used across welds in view of the possibility of a local plastic failure if deep local deviations occur as shown in Fig. 13(b).

The measured imperfections are made dimensionless as

$$U_{0x} = \frac{\Delta w_{0x}}{L_{gx}}, \quad U_{0w} = \frac{\Delta w_{0w}}{L_{gw}} \tag{13}$$

and the values of $U_0$ are limited to fall below the tolerance $U_{0,\max}$. The gauges are devised so as to be related to the size of buckles that are expected to form under each of the different basic load cases. The length is chosen in the light of the sensitivity of buckling strengths to imperfections in the form of the lowest classical eigenmode. This may not be the most serious imperfection, but it is one of the most serious, so it provides a moderately good control (Rotter and Schmidt 2008).

The value of the $U_{0,max}$ depends on the fabrication accuracy and three different fabrication

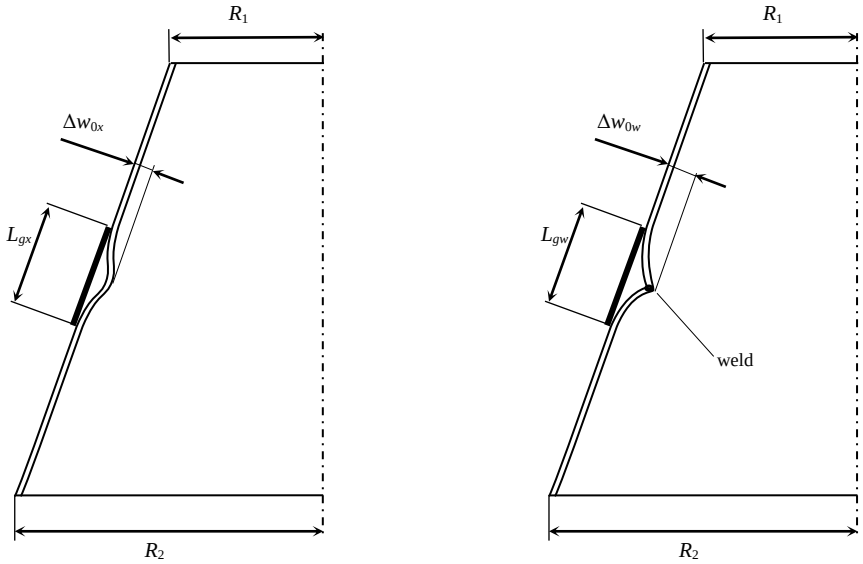


(a) Measurement on a meridian (b) Additional measurement across a weld

Fig. 13 Measurement of depths $\Delta_{w0}$ of initial dimples

Table 4 Values for imperfection tolerance $U_{0,max}$ and quality parameter $Q$ (Teng and Rotter 2004)

| Fabrication tolerance quality class | Description | Value of $U_{0,max}$ | $Q$ |
|---|---|---|---|
| Class A | Excellent | 0.006 | 40 |
| Class B | High | 0.01 | 25 |
| Class C | Normal | 0.016 | 16 |

quality classes are defined, as indicated in Table 4, allowing highly controlled fabrication to exploit the highest strength, but allowing less controlled construction to assume a lower buckling load.

### *3.4 Hand Calculation rule to accounting for imperfection effects*

In the design of conical shells, following the ECCS (Rotter and Schmidt 2008) (see section 10.2) and after adapting the equations to cones by using the lowest radius of curvature, the characteristic imperfection amplitude $\Delta w_x$ is

$$\Delta w_x = \frac{1}{Q}\sqrt{\frac{\rho_1}{t}}t \tag{14}$$

where $Q$ is the meridional compression fabrication quality parameter reported in Table 4.

## 4. Imperfection sensitivity of cones and implications to their buckling design

In the light of the above, it is clear that different forms of imperfections have different effects,

so both the form and the amplitude must be considered to be used in design applications. To this end, the following two alternatives can be pursued

1. Finding the 'worst' imperfection pattern;
2. Applying the theoretical lower bound strength that makes the design independent of the form and amplitude of imperfections

### *4.1 The 'worst' imperfection pattern*

This approach seeks to identify the worst imperfection mode, and has the advantage that the search is formal and mathematical, so it is potentially achievable provided that the problem statement and failure criteria have sufficient generality. It has the great advantage that, potentially, it can be generalized for all shell forms and load cases, so problems can be studied for which no test data exist (as in most real design configurations) (Teng and Rotter 2004).

The most widely used interpretation of this concept is that an imperfection in the form of the linear bifurcation (buckling) modes of the perfect shell is close to the worst form. Teng and Song (Teng and Song 2001) discussed about a number of issues that needs particular care in nonlinear finite element analysis of elastic shells with eigenmode (linear buckling mode) imperfections and tackled some recommendations about four different kinds of models. Deml and Wunderlich (1997) developed a fully nonlinear finite element method for the evaluation of the imperfection-sensitivity of elastic and elastic-plastic shells that directly gives the 'worst' imperfection shape connected to the ultimate limit load.

### *4.2 Theoretical lower bounds on strength*

In this approach, the goal is to find lower bounds on the strengths of the shell using the results obtained from theoretical analyses. Using this approach makes the design process free from concerns about the form and amplitude of the imperfections and the problems of tolerance measurement and control are greatly reduced. This approach was formerly used by Esslinger and Geier (1976), Croll and Ellinas (1985), Yamada and Croll (1999) for cylindrical shells, but to the authors' knowledge, it is not adopted for the conical shells yet.

#### *4.2.1 Finding the lower bound for conical shells*

Fig. 14 shows the imperfection sensitivity of the cone with all imperfection forms and tapering angles being considered. It can be seen that the weld depression (located in the middle of the cone), has the less effect on the buckling load and the lower bound of imperfection sensitivity of cones is approximately from FALB mode. The lower bound curve, based on the minimum values of load factors in any imperfection amplitude is also shown in Fig. 14.

The characteristic imperfection is then used to find an empirical relationship for the elastic buckling strength ($\alpha_x$) dependency on relative imperfection amplitude ($\Delta w_x/t$) that is in the form of

$$\alpha_x = \frac{0.75}{1+1.40(\Delta w_x/t)^{0.55}} \tag{15}$$

The above imperfection amplitude is also shown in Fig. 14. Using Eq. (15), the designers can be guaranteed that all types of imperfection shapes are considered in their designs.

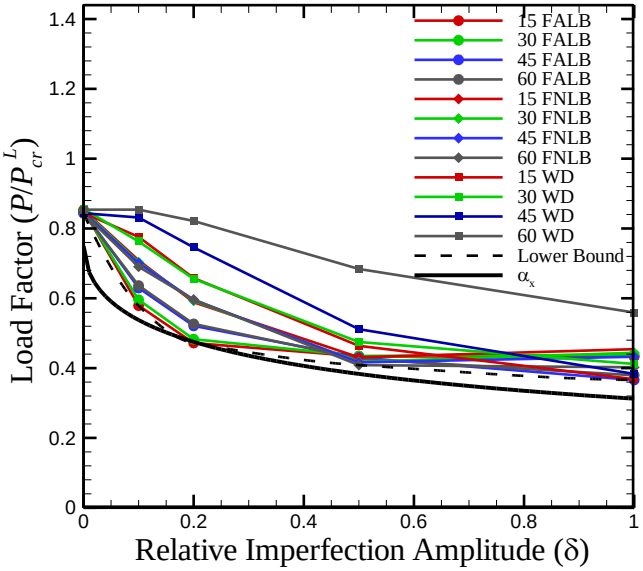


Fig. 14 Summary of imperfection sensitivity curves of cones for different types of imperfections

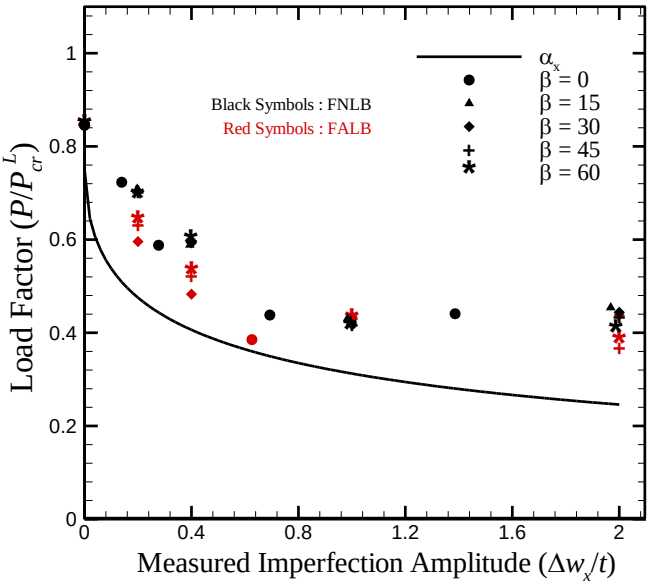


Fig. 15 The measured imperfection values and the $\alpha_x$ curve for FNLB and FALB types of imperfections

### *4.3 Rescaling of amplitudes*

An important point of view about all above graphs is that the imperfection amplitudes are referred to the deviation from the nominal geometry. However, as described in section 3.3, when the imperfections are measured on-site, a ruler is used which has a certain length and the

amplitudes of imperfections are measured as the deviation from the ruler which is placed on the imperfect shell wall. This means that there is a difference between the mathematical amplitude of imperfection and that measured with the gauge. Since the function describing imperfection shape is known (see Table 3 for meridional wave numbers), the relation between imperfection amplitude measured with the ruler and that corresponding to deviation from nominal geometry can be obtained analytically.

Fig. 15 shows the imperfection sensitivity curve and the elastic buckling strength for the cone, where the $x$ axis is the measured imperfection amplitude obtained for FNLB and FALB imperfection forms. This figure ensures that the elastic buckling strength ($\alpha_x$) introduced in Eq. 15 is a good relation between the elastic imperfection reduction and the measured imperfection amplitudes.

## 5. Conclusions

The imperfection sensitivity of conical shells under axial compression is thoroughly estimated for three different imperfection shapes through FE nonlinear analyses, having in mind the theoretical curves for the cylindrical counterparts. It is shown that there is little influence of the tapering angle of cone on the imperfection sensitivity and that imperfections of shape corresponding to the first axisymmetric bifurcation modes seem to be the most detrimental among the ones being investigated. All the imperfection curves for cones tend to stabilize as imperfection amplitude increases. This seems to occur when the imperfection bulge fully develops under loading along the length of the shell (this trend is particularly evident for weld depression). Such stabilized imperfection sensitivity curves for cones appear to deviate from those of cylinders (and from the theoretical curves, related to cylinders of infinite length, due to Koiter and Yamaki), where this kind of saturation in the imperfection bulge under loading is less likely to occur (note that in cones the condition of infinite length can never be achieved as the slant length is governed by the $R_2/R_1$ ratio and the tapering angle $\beta$). On the basis of the whole set of results obtained from FE nonlinear analysis, a lower bound expression of the knock-down factor for cones, in a form compatible with current buckling design recommendations, is proposed.

## References

Ac Shiau, R.R. and Soong, T. (1974), "Dynamic buckling of conical shells with imperfections", *AIAA J.*, **12**(6), 755-760.

Ali, L., Jalal, E.B., Abdellatif, K. and Larbi, E.B. (2011), "Effect of multiple localized geometric imperfections on stability of thin axisymmetric cylindrical shells under axial compression", *Int. J. Solid. Struct.*, **48**(6), 1034-1043.

Association, A.W.W. (1984), "ANSI/AWWA D100-84, Standard for Welded Steel Tanks for Water Storage", Denver, Colo.: AWWA.

Batista, R. and Croll, J. (1980), *A design approach for unstiffened cylindrical shells under external pressure*, John Wiley and Sons, Inc.

Berry, P., Rotter, J. and Bridge, R. (2000), "Compression Tests on Cylinders with Circumferential Weld Depressions", *J. Eng. Mech.*, **126**(4), 405-413.

BŁachut, J. (2011), "On elastic-plastic buckling of cones", *Thin Wall. Struct.*, **49**(1), 45-52.

Calladine, C. (1995), "Understanding imperfection-sensitivity in the buckling of thin-walled shells", *Thin*

*Wall. Struct.*, **23**(1), 215-235.
Castro, S.G.P., Zimmermann, R., Arbelo, M.A., Khakimova, R., Hilburger, M.W. and Degenhardt, R. (2014), "Geometric imperfections and lower-bound methods used to calculate knock-down factors for axially compressed composite cylindrical shells", *Thin Wall. Struct.*, **74**, 118-132.
Chaudhuri, R.A. and Kim, D. (2008), "Influence of localized imperfection and surface-parallel shear modulus nonlinearity on the instability of a thin cross-ply cylindrical shell under external pressure", *Compos. Struct.*, **82**(2), 235-244.
Chryssanthopoulos, M., Pariatmono, N. and Spagnoli, A. (1997). "Buckling tests of unstiffened and stiffened conical shells in compression", *Proceedings, International Conference on Carrying Capacity of Steel Shell Structures*, V. Krupka and P. Schneider, eds., October.
Croll, J. and Ellinas, C. (1985), "A design formulation for axisymmetric collapse of stiffened and unstiffened cylinders", *J. Energy Res. Technol.*, **107**(3), 350-355.
Croll, J.G. (1995), "Towards a rationally based elastic-plastic shell buckling design methodology", *Thin Wall. Struct.*, **23**(1), 67-84.
Deml, M. and Wunderlich, W. (1997), "Direct evaluation of the 'worst' imperfection shape in shell buckling", *Comput. Meth. Appl. Mech. Eng.*, **149**(1-4), 201-222.
Ding, X., Coleman, R. and Rotter, J. (1996), "Technique for Precise Measurement of Large-Scale Silos and Tanks", *J. Surv. Eng.*, **122**(1), 14-25.
Donnell, L. and Wan, C. (1950), "Effects of imperfections on buckling of thin cylinders and columns under axial compression", *J. Appl. Mech.*, **17**(1), 73.
Esslinger, M. and Ciprian, J. (1982), *Buckling of thin conical shells under axial loads with and without internal pressure*, Springer
Esslinger, M. and Geier, B. (1976), *Calculated postbuckling loads as lower limits for the buckling loads of thin-walled circular cylinders*, Springer
Falzon, B.G. and Aliabadi, M.H. (2008), *Buckling and postbuckling structures: experimental, analytical and numerical studies*, Imperial College Press
Ghazijahani, T.G., Jiao, H. and Holloway, D. (2015), "Experiments on locally dented conical shells under axial compression", *Steel Compos. Struct.*, **19**(6), 1355-1367.
Goldfeld, Y. (2007), "Imperfection sensitivity of laminated conical shells", *Int. J. Solid. Struct.*, **44**(3-4), 1221-1241.
Holst, J.M.F.G., Rotter, J.M. and Calladine, C.R. (2000), "Imperfections and buckling in cylindrical shells with consistent residual stresses", *J. Constr. Steel Res.*, **54**(2), 265-282.
Hutchinson, J. and Koiter, W. (1970), "Postbuckling theory", *Appl. Mech. Rev*, **23**(12), 1353-1366.
Jalili, S., Zamani, J., Shariyat, M., Jalili, N., Ajdari, M. and Jafari, M. (2014), "Experimental and numerical investigation of composite conical shells' stability subjected to dynamic loading", *Struct. Eng. Mech.*, **49**(5), 555-568.
Jamal, M., Lahlou, L., Midani, M., Zahrouni, H., Limam, A., Damil, N. and Potier-Ferry, M. (2003), "A semi-analytical buckling analysis of imperfect cylindrical shells under axial compression", *Int. J. Solid. Struct.*, **40**(5), 1311-1327.
Jamal, M., Midani, M., Damil, N. and Potier-Ferry, M. (1999), "Influence of localized imperfections on the buckling of cylindrical shells under axial compression", *Int. J. Solid. Struct.*, **36**(3), 441-464.
Koiter, W. (1963). "The effect of axisymmetric imperfections on the buckling of cylindrical shells under axial compression", *Koninkl. Ned. Akad. Wetenschap. Proc. B.*
Koiter, W. (1970), *On the stability of elastic equilibrium (Translation from Dutch)*, Tech. Rep. AFFDL-TR-70-25, Airforce Flight Dynamics Lab
Koiter, W.T. (1970), *The stability of elastic equilibrium*, DTIC Document
Koiter, W.T. and Heijden, A.M.A. (2009), *W.T. Koiter's elastic stability of solids and structures*, Cambridge University Press
Lackman, L. and Penzien, J. (1960), "Buckling of circular cones under axial compression", *J. Appl. Mech.*, **27**, 458.
Lawrence, K.L. (2012), *ANSYS Tutorial: Release 14*, SDC Publications

Maali, M., Showkati, H. and Mahdi Fatemi, S. (2012), "Investigation of the buckling behavior of conical shells under weld-induced imperfections", *Thin Wall. Struct.*, **57**, 13-24.
Muggeridge, D. and Tennyson, R. (1969), "Buckling of axisymmetric imperfect circular cylindrical shells underaxial compression", *AIAA J.*, **7**(11), 2127-2131.
Norm, D. (1990), *Structural steelwork: analysis of safety against buckling of shells, DIN 18800 part 4*, German Institute for Standardization, Berlin.
Pariatmono, N. and Chryssanthopoulos, M. (1995), "Asymmetric elastic buckling of axially compressed conical shells with various end conditions", *AIAA J.*, **33**(11), 2218-2227.
Peterson, J., Seide, P. and Weingarten, V. (1968), NASA SP-8007: Buckling of thin-walled circular cylinders.
Pircher, M., Berry, P.A., Ding, X. and Bridge, R.Q. (2001), "The shape of circumferential weld-induced imperfections in thin-walled steel silos and tanks", *Thin Wall. Struct.*, **39**(12), 999-1014.
Riks, E. (1979), "An incremental approach to the solution of snapping and buckling problems", *Int. J. Solid. Struct.*, **15**(7), 529-551.
Rotter, J. (1996). "Elastic plastic buckling and collapse in internally pressurised axially compressed silo cylinders with measured axisymmetric imperfections: interactions between imperfections, residual stresses and collapse", *Proceedings of the International Workshop on Imperfections in Metal Silos: Measurement, Characterisation and Strength Analysis*, CA-Silo, Lyon, France.
Rotter, J. and Teng, J. (1989), "Elastic Stability of Cylindrical Shells with Weld Depressions", *J. Struct. Eng.*, **115**(5), 1244-1263.
Rotter, J.M. and Schmidt, H. (2008), *ECCS TWG 8.4. Buckling of steel shells*, 5th Edition, European convention for constructional steelwork, Brussels.
Schultz, M.R. and Nemeth, M.P. (2010), "Buckling imperfection sensitivity of axially compressed orthotropic cylinders", *AIAA J.*, **2531**.
Shakouri, M., Spagnoli, A. and Kouchakzadeh, M.A. (2014), "Re-interpreting simultaneous buckling modes of axially compressed isotropic conical shells", *Thin Wall. Struct.*, **84**, 360-368.
Sofiyev, A.H. (2011), "Influence of the initial imperfection on the non-linear buckling response of FGM truncated conical shells", *Int. J. Mech. Sci.*, **53**(9), 753-761.
Song, C.Y., Teng, J.G. and Rotter, J.M. (2004), "Imperfection sensitivity of thin elastic cylindrical shells subject to partial axial compression", *Int. J. Solid. Struct.*, **41**(24-25), 7155-7180.
Spagnoli, A. (2001), "Different buckling modes in axially stiffened conical shells", *Eng. Struct.*, **23**(8), 957-965.
Spagnoli, A. (2003), "Koiter circles in the buckling of axially compressed conical shells", *Int. J. Solid. Struct.*, **40**(22), 6095-6109.
Spagnoli, A. and Chryssanthopoulos, M.K. (1999), "Elastic buckling and postbuckling behaviour of widely-stiffened conical shells under axial compression", *Eng. Struct.*, **21**(9), 845-855.
Standard, A. (1977), *Recommended Rules for Design and Construction of Large, Welded, Low−Pressure Storage Tanks*, API.
Teng, J. and Rotter, J. (1992), "Buckling of pressurized axisymmetrically imperfect cylinders under axial loads", *J. Eng. Mech.*, **118**(2), 229-247.
Teng, J.G. and Rotter, J.M. (2004), *Buckling of thin metal shells*, Spon Press
Teng, J.G. and Song, C.Y. (2001), "Numerical models for nonlinear analysis of elastic shells with eigenmode-affine imperfections", *Int. J. Solid. Struct.*, **38**(18), 3263-3280.
VonKarman, T. and Tsien, H.-S. (1941), "The buckling of thin cylindrical shells under axial compression", *J. Aeronaut. Sci.*, **8**(8), 303.
Yamada, S. and Croll, J. (1999), "Contributions to understanding the behavior of axially compressed cylinders", *J. Appl. Mech.*, **66**(2), 299-309.
Yamaki, N. (1984), *Elastic Stability of Circular Cylindrical Shells*, Elsevier Science